

# RADIOMETRIC PERFORMANCE REQUIREMENTS FOR OPTIMAL ATMOSPHERIC PROCESSING OF HYPERSPECTRAL IMAGERY

D. Schläpfer, S. Bojinski, and M. Schaepman

Remote Sensing Laboratories, RSL  
University of Zurich, Winterthurerstr. 190, CH-8057 Zürich  
dschlapf@geo.unizh.ch

**KEY WORDS:** Atmospheric signatures, oxygen, water vapor, sensitivity analysis

## ABSTRACT

The radiometric performance of an hyperspectral sensor is limited due to physical constraints such as quantization, noise levels, spectral resolutions, and calibration accuracy. During the definition phase of a hyperspectral instrument, these numbers have to be defined based on scientific requirements for atmospheric correction methods to be applied and with respect to a variety of hyperspectral applications and data products. This paper describes these requirements with respect to the measurement of atmospheric constituents such as water vapor, oxygen, and aerosols. These parameters all are relevant for the optimal performance of atmospheric correction procedures. Requirements for delta radiance detectability and spectral calibration accuracy are derived from straightforward radiative transfer modelling. The results prove that highest quality hyperspectral instruments are required for a reliable quantitative analysis of atmospheric signatures.

## 1 INTRODUCTION

The design of hyperspectral instruments is very critical with regard to their technical specifications. Overspecifying a system will lead to exhaustive costs whereas underspecifying will leave room for ambiguities. In some cases, the scientific requirements are not defined well enough but in most cases they cannot be easily transferred to engineering specifications. Sensitivity analyses using physical models are therefore absolutely required for all anticipated applications of the hyperspectral imagery. Atmospheric constituents can potentially be retrieved from imaging spectrometer data based on physical models. The resulting atmospheric parameters are of major interest for pixelwise atmospheric correction procedures.

The goal of this contribution is to define the order of magnitude for radiometric performance numbers such as radiometric resolution and calibration accuracy. More accurate limits can only be given if sophisticated sensor models (Börner et al., 1999) are used and if clear limits for parameter detectability are defined. The analysis is done with respect to three atmospheric parameters knowing that similar studies are required for land surface processes and water body analysis for a profound definition of radiometric requirements throughout the wavelength range covered by the spectrometer.

The following analysis concentrates on the pure radiometric effects of the atmospheric parameters on the at-sensor signal. The derived numbers describe a baseline of requirements to hyperspectral instruments if quantitative results are called for. The methodology for the evaluation of this signal is not considered – sophisticated methods of parameter retrieval are required for a reliable exploitation of this signal.

## 2 SENSITIVITY ANALYSIS

The sensitivity analysis is performed for three types of atmospheric constituents: Water vapor, oxygen, and aerosols. The applied algorithm first resolves typical variations of these constituents within hyperspectral images and then models the respective signatures using the MODTRAN radiative transfer code (Berk et al., 1989). Given some typical requirements on the detectability of the individual atmospheric constituents, recommendations on the required sensor performance can be made. The detection thresholds for the constituents are defined based on the requirements for atmospheric correction and the experience of the authors in atmospheric correction and parameter retrieval.

### 2.1 Water Vapor

Water vapor is among the main atmospheric gases influencing the hyperspectral signal. Its correct retrieval is crucial for atmospheric correction of the full spectral range. The sensitivity of an imaging spectrometer to the columnar water vapor content is high throughout a large number of spectral bands while the most commonly used absorption feature is situated at 940 nm. The required noise levels as well as the influence of spectral mis-registration within this absorption feature are described first. Some extensive sensitivity analyses and a methodology for the retrieval of water vapor from imaging spectrometry data have already been presented by Schläpfer (1998).

**2.1.1 Radiometric Resolution.** The water vapor partial column which is relevant for meteorological applications is in the range of 0.05-0.2 g/cm<sup>2</sup> column Precipitable Water (PW). Such in-scene variations have been reported within areas covered by hyperspectral images and are significantly influencing the hyperspectral signal (Schläpfer, 1998). The radiometric signal equivalent to the 0.05 g/cm<sup>2</sup> column water vapor has been derived in the 940 nm water vapor absorption feature using MODTRAN simulations at total water vapor contents between 0.5 and 4 g/cm<sup>2</sup>. Thus, the above given absolute water vapor variations corresponds to a relative water vapor retrieval error of 1.25 - 10%.

The convolution of the simulated spectra has been performed to Gaussian band function with a) varying FWHM between 2 and 40 nm and b) varying band center from 920 to 960 nm at 10 nm FWHM resolution.

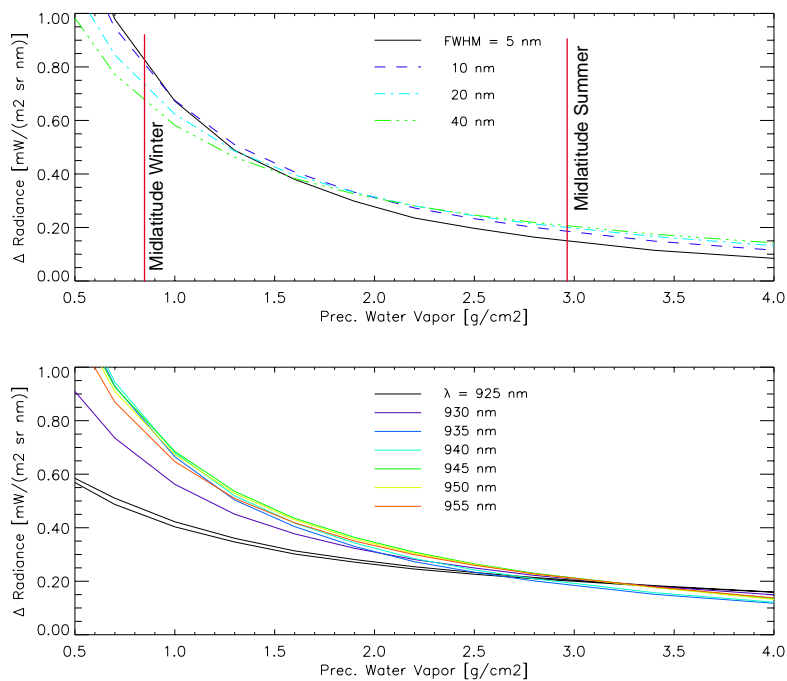


Figure 1: Radiometric requirement for detection of a column water vapor difference of 0.05 g/cm<sup>2</sup> for pixelwise applications at various water vapor levels.

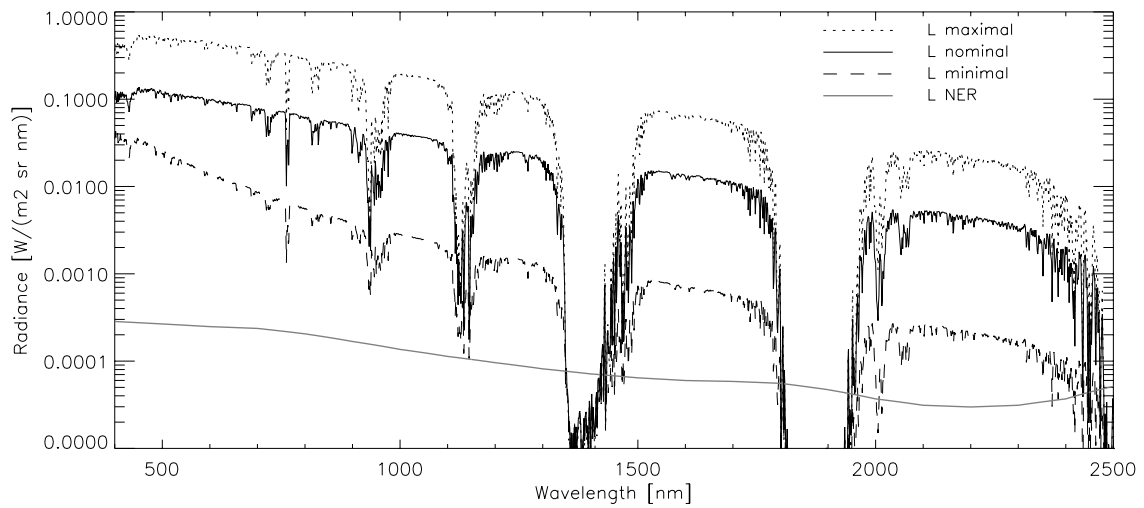


Figure 2: Proposed radiometric performance requirements for a future hyperspectral sensor derived from optimized performance numbers of existing systems.

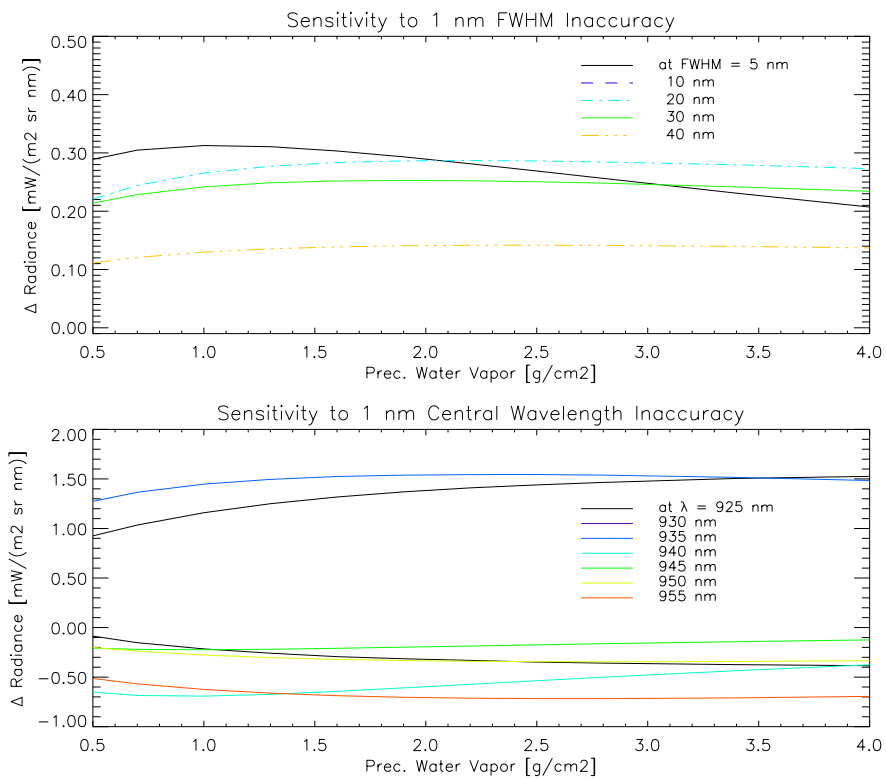


Figure 3: Sensitivity to spectral mis-calibrations for FWHM and Band Center Position in the water vapor absorption feature.

The resulting radiometric requirements are depicted in Figure 1. For both analysis series, the critical NEdL has been derived being at  $0.1 \text{ mW}/(\text{m}^2 \text{ sr nm})$ . The retrieval is more critical at high water vapor contents, where the water vapor absorption tends to saturate. However, this limit is only valid for the 940 nm range and for the water vapor case. The level of delta radiance is in good agreement to the NEdL performance of hyperspectral instruments as shown in Figure 2 (ESA, 2000).

**2.1.2 Spectral Calibration.** The spectral requirements in the 940 nm water vapor absorption region are mainly driven by the strong absorption slopes of the feature. The effect of spectral miscalibrations has been investigated based on 1 nm steps in band center position and width (at FWHM). The resulting delta radiances as given in Figure 3 can be linearly reduced to obtain an estimate of the errors for smaller calibration errors.

First, the FWHM has been changed by steps of 1 nm. The resulting delta radiances are low, between 0.1 and 0.3 mW/(m<sup>2</sup> sr nm). We conclude, that an accuracy of ±0.5 nm in FWHM would be enough for the errors of water vapor retrieval remain below the limits as given in the section above. This influence of bandwidth is apparently not as critical for the water vapor feature since the absorption feature spreads over about 100 nm and the evaluation band has been taken in the band center.

Secondly, the spectral position has been changed. Here, the observed delta radiances are much higher than for the bandwidth variation. The related larger errors imply that the spectral position has to be known to the extent of 0.1 to 0.2 nm accuracy, to remain within the detectable limits. Such accuracy in calibration is very stringent but obviously required for the proper analysis of the water vapor amount. Spectral calibration requirements in the same order of magnitude have also been reported by Green (1998).

## 2.2 The Oxygen Band at 762 nm

Another feature of importance is the narrow-band oxygen absorption at 762 nm (compare Figure 4). Due to its sharp absorption characteristics, it can help to retrieve aerosol contents as well as to calibrate the wavelength accuracy and to derive terrain elevation from the imagery itself. Its spectral sharpness drives the requirements for spectral resolution and spectral position knowledge at this wavelength. The required resolution for the exploration of this feature is defined. Its anticipated detectability limit is set to 30 m column at sea level altitude (at 7500 m total column). This number is corresponding to the optical path length which is relevant for atmospheric correction purposes as it can be experienced when performing atmospheric corrections in mountainous terrain.

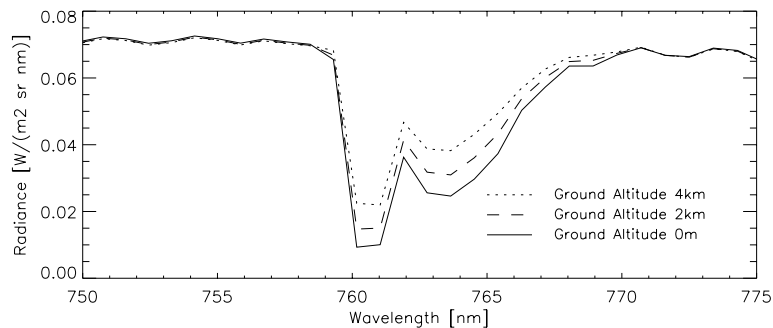


Figure 4: The Oxygen absorption feature at 762 nm modeled at 1 nm resolution. Its width is between 5 and 7 nm (MODTRAN 4 / MODO output).

**2.2.1 Spectral Resolution.** The influence of the spectral resolution on the oxygen detectability has been tested. A model was set up, where the radiance difference at various ground altitudes has been compared to the noise equivalent delta radiance of 0.1 mW/(m<sup>2</sup> sr nm) (as derived in the section above). The inversion of the procedure allows to investigate on the detectability of the oxygen column which corresponds directly to the ground altitude. The results of these tests are shown in Figure 6. A columnar oxygen amount equivalent to 100 m elevation difference can be measured at best resolution of 5 nm. The sensitivity drops exponentially while decreasing spectral resolution. At 8 nm (FWHM) it is still acceptable (corresponding to 150 m column) but as the resolution decreases further, the observed signal becomes less significant. The theoretical radiometric requirement for pixelwise oxygen retrieval would be at 0.02 mW/(m<sup>2</sup> sr nm) at 8 nm FWHM resolution. To increase accuracy, the at-sensor spectra may be spatially averaged. The considered critical vertical column of

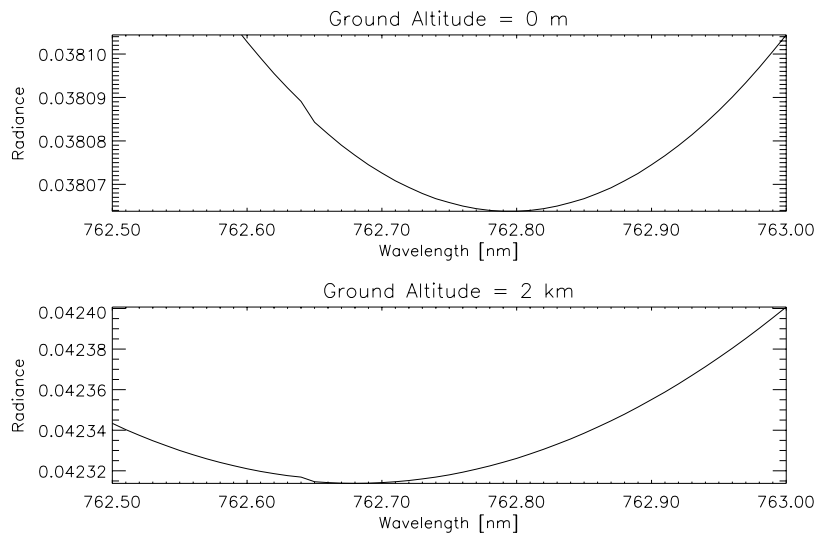


Figure 5: Spectral position of the oxygen absorption feature and radiance errors at spectral mis-calibrations of 0.3 nm and FWHM = 7.5 nm.

30 m oxygen can thus be retrieved by applying a 5 x 5 pixels spatial averaging algorithm and having a sensor with 8 nm spectral resolution and 0.1 mW(m<sup>2</sup> sr nm) radiometric resolution.

**2.2.2 Spectral Calibration Accuracy.** The oxygen absorption feature may also be taken as reference wavelength for adjusting the spectral position of the detector array. The feature absorption maximum has therefore to be defined exactly. The central position of the band was searched at a resolution of FWHM = 7.5 nm between 760 and 765 nm based on the standard MODTRAN at-sensor radiance values. The result (see Figure 5) shows a slight shift of the central wavelength position from 762.8 nm to 762.7 nm and lower, depending on the ground altitude. This shift originates from the change of the aerosol scattering function with altitude. We conclude to fix the position of the reference spectral band at an average oxygen band position of 762.75 nm. This analysis again points out a spectral position calibration accuracy requirement in the range of 0.1 nm.

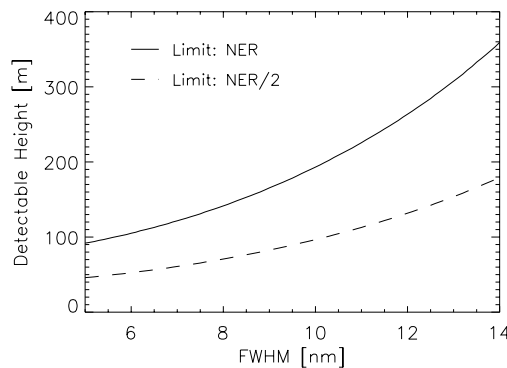


Figure 6: Detectability of oxygen column height differences dependent on the spectral resolution at FWHM.

### 2.3 Aerosols

In this part, we present a sensitivity analysis of the spectral signal for a variety of standard aerosol models using the MODTRAN radiative transfer code. The goal is to assess the influence of the type of aerosol and aerosol abundance, expressed by the visibility, on the visible and near-infrared wavelength range spectral signal. The visibility has been taken as driving parameters for aerosol optical thickness in analogy to the imple-

mentation of the MODTRAN code. Based on at-sensor radiance simulations, we derive the minimal noise equivalent delta radiance (NE $\Delta$ L) of the sensor that is required for the distinction of the different spectral signatures.

The aerosol contents mainly influence the signal in the short wavelengths between 400 to 1000 nm due to their varying scattering impact. The signatures can therefore be investigated with respect to sensor specifications in a wavelength ranges which are often critical in the Signal to Noise ratio, due to the performance decrease of Silicon detectors towards both ends of this wavelength range.

The distinction between typical rural, maritime, and urban type is chosen as minimal requirement to be retrieved. For simplicity, uniform surface reflectances  $\rho = 0.0$  and  $\rho = 0.3$  are assumed. The MODTRAN RT code is run for a mid-latitude summer and Central European scenario for a sensor altitude of 7.5 km, with visibilities varying from 5 to 50 km and with these three discrete aerosol models.

**2.3.1 Aerosol Type.** The difference in spectral signatures of various aerosol types is significant as depicted in Figure 7 (top). Experience shows that for a typical hyperspectral analysis, a distinction of aerosol optical thickness between 10 and 11 km visibility is desired. Therefore, the differences in spectral magnitude between the 10 km and the 11 km case for the three aerosol types are simulated and evaluated, as shown in Figure 7. For  $\rho = 0.0$ , the spectral effect of visibility variation is smaller for urban aerosols than for the rural and maritime case, but for the most part exceeds 0.5 mW/(m<sup>2</sup> sr nm) in the investigated wavelength range. For  $\rho = 0.3$  (compare Figure 8), a different scattering and absorption regime prevails, as the delta radiance tends to negative values (Asrar, 1989). The signal variation magnitudes for the urban case float between 1 and 4 mW/(m<sup>2</sup> sr nm), close to 0.5 for the rural (see Figure 11), and around 1 mW/(m<sup>2</sup> sr nm) for the maritime aerosol type.

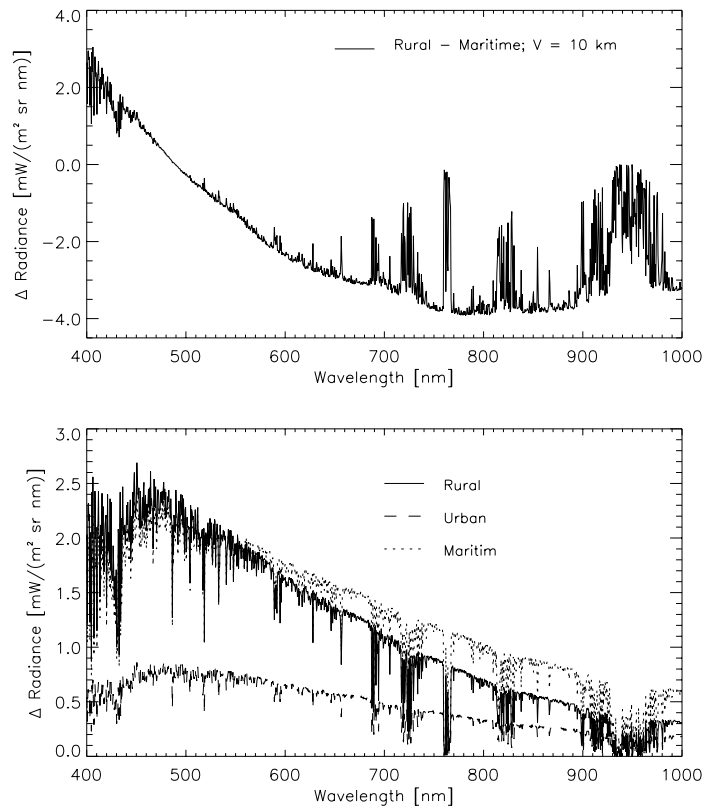


Figure 7: Differences between rural and Maritime aerosol model (top) and differences between at-sensor radiance from 10 km to 11 km visibility and different aerosol types for  $\rho = 0.0$ .

**2.3.2 Aerosol Optical Thickness.** The visibility variation of 1 km at  $V = 10$  km corresponds to a change  $\Delta\tau_0$  in optical thickness, an atmospheric parameter which is, for not too strong multiple scattering, roughly inverse proportional to the visibility. For a proper comparison of the spectra,  $\Delta\tau_0$  is applied for different atmospheric conditions, namely for visibilities of 5, 23, and 50 km, resulting in different increments of visibility variation. Figure 9 depicts the differential radiances for a rural aerosol type and  $\rho = 0.0$ . Bar the  $V = 5$  km case, the curves behave as expected and match quite well, in a delta radiance range of 1 to 3  $\text{mW}/(\text{m}^2 \text{sr nm})$ . In the former, the inverse proportionality assumption no longer holds due to multiple scattering. Again, the  $\rho = 0.3$  counterpart (Figure 10) displays a different, less spiky behaviour of the delta radiance in a different scattering regime, which barely exceeds 1  $\text{mW}/(\text{m}^2 \text{sr nm})$ .

In this part, the MODTRAN simulated spectral signal variation due to different aerosol types and visibilities has been investigated. To conclude, a minimum sensor signal resolution (NE $\Delta$ L) of 0.5  $\text{mW}/(\text{m}^2 \text{sr nm})$  is required to discern a change in the spectral signal caused by a visibility variation of 1 km at 10 km or an equivalent optical thickness change.

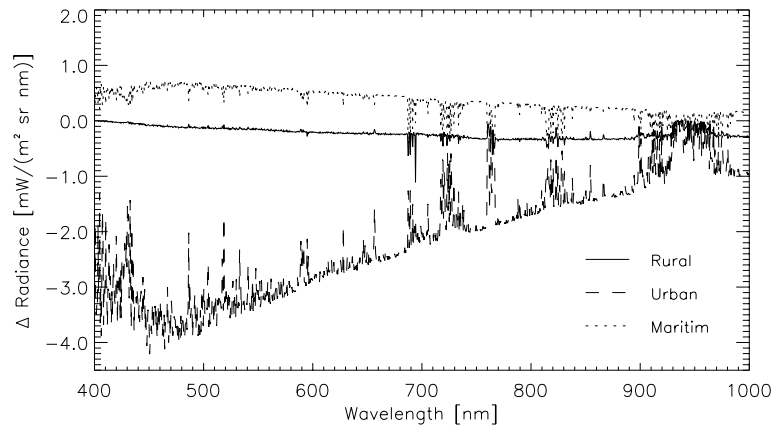


Figure 8: Differences between at-sensor spectral magnitudes for 10 km and 11 km visibility and different aerosol types for  $\rho = 0.3$ .

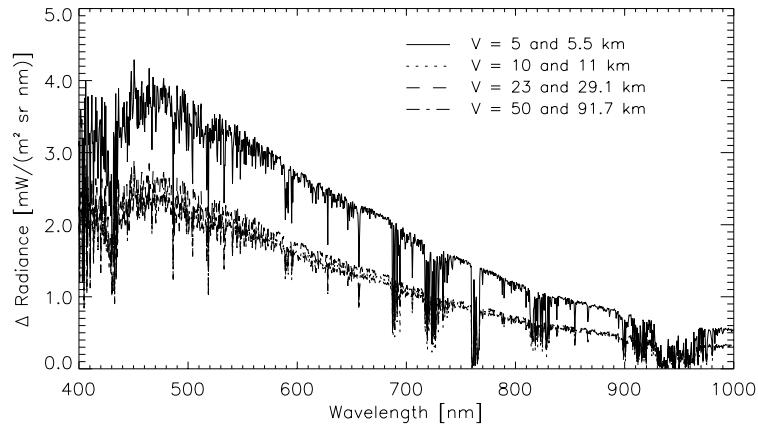


Figure 9: Differences between at-sensor spectral magnitudes for visibilities 5, 10, 23, and 50 km and the respective higher visibilities corresponding to the change in optical thickness between the 10 km and the 11 km case. Rural aerosol type for  $\rho = 0.0$ .

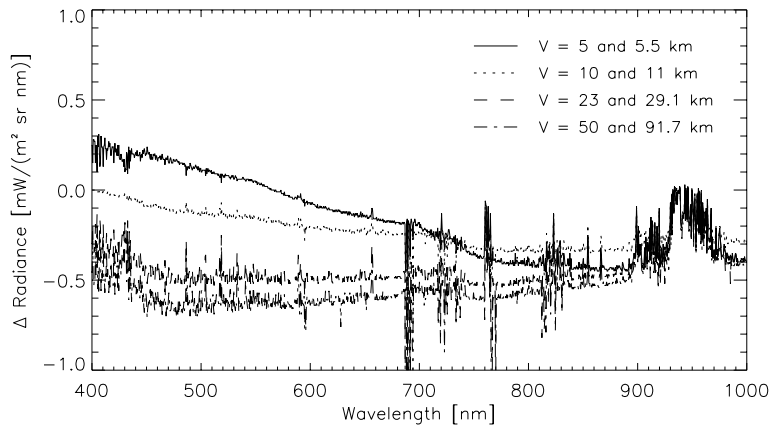


Figure 10: Differences between at-sensor spectral magnitudes for visibilities 5, 10, 23, and 50 km and respective higher visibilities corresponding to the change in optical thickness between the 10 km and the 11 km case. Rural aerosol type for  $\rho = 0.3$ .

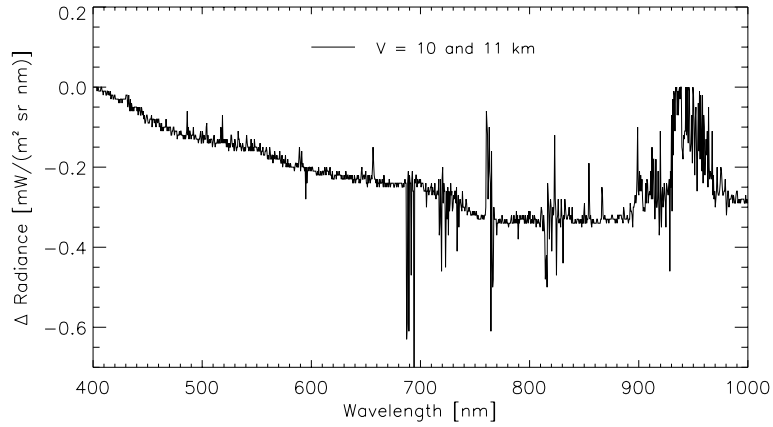


Figure 11: Differences between at-sensor spectral magnitudes for the 10 km and 11 km case visibilities. Rural aerosol type for  $\rho = 0.3$ . The simulation with MODTRAN applies to a mid-latitude summer atmospheric model and central European coordinates for a sensor altitude of 7.5 km

### 3 CONCLUSIONS

General requirements for radiometric performance have been formulated with respect to the atmospheric measurement capabilities of a generic hyperspectral instrument in the visible and near infrared part of the spectrum. The critical radiometric resolution (NE $\Delta$ L) has been found to be between 0.1 and 0.5 mW/(m<sup>2</sup> sr nm) consistently for all three evaluated parameters. Based on the shapes of the main gaseous absorption feature characteristics an ideal spectral resolution of 6 to 10 nm can be recommended. For the same level of errors, the spectral calibration accuracy has to be between 0.1 and 0.3 nm.

The figures found for aerosol signatures are more relaxed than those found from gaseous absorption signatures. It must be noted though, that a strong dependence of the delta radiances on the background surface reflectance has been observed. Under natural conditions, this calls for a far higher radiance sensitivity of the sensor that is employed for the retrieval of atmospheric parameters. We can therefore assume that strict NE $\Delta$ L sensor specifications are certainly of high benefit for a thorough analysis of atmospheric effects on at-sensor spectra.

The requirements as given from the atmospheric application point of view are in good agreement to the capabilities of current and planned state-of-the-art imaging spectrometers. Anyhow, only atmospheric signatures have been investigated so far which affected the visible and near infrared part of the spectrum. In future work, the requirements to hyperspectral sensors have also to be exhaustively evaluated against land and water applications where similar modelling approaches will lead to radiometric requirements for the whole wavelength range.

#### 4 ACKNOWLEDGEMENTS

We acknowledge the support through ESA/ESTEC Contract No. 13115/98/NL/VJ(IC) [APEX Phase B]. In particular the support of Roland Meynard from ESA/ESTEC is acknowledged.

#### REFERENCES

- Asrar G., 1989: *Theory and Applications of Optical Remote Sensing*, Wiley, New York.
- Berk A., Bernstein L.S., and Robertson D.C., 1989: *MODTRAN: A Moderate Resolution Model for LOWTRAN7*. Air Force Geophysics Laboratory, Hanscom AFB, MA, GL-TR-89-0122, pp 38.
- Börner A., Schaepman M., Schläpfer D., Wiest L., and Reulke R., 1999: The Simulation of APEX Data: The SENSOR approach. *Imaging Spectrometry V*, Denver, SPIE Vol. **3753**:235-246.
- ESA, 2000: *APEX Phase B Final Reports*, CD-Rom, Remote Sensing Laboratories, Univ. of Zurich, Switzerland
- Gao B.-C., and Kaufmann Y.J., 1993: Remote Sensing of Smoke, Clouds and Fire Using AVIRIS Data. Green R. (Ed.) (Ed.), *Summaries of the Fourth Annual JPL Airborne Geoscience Workshop*, JPL California Institut of Technology, Pasadena, Vol. 1, pp 61 - 64.
- Green R.O., 1998: Spectral calibration requirement for Earth-looking imaging spectrometers in the solar-reflected spectrum. *Appl. Optics*, OSA, **37(4)**:683-690.
- Kaufman Y.J., 1987: Satellite Sensing of Aerosol Absorption. *J. of Geophysical Research*, **92(D4)**:4307 - 4317.
- Kaufman Y.J., and Tanré D., 1996: Strategy for Direct and Indirect Methods for Correction the Aerosol Effect on Remote Sensing: From AVHRR to EOS-MODIS. *Remote Sens. Environ.*, **55**:65-79.
- King M.D., Kaufmann Y.J., Menzel W.P., and Tanré D., 1992: Remote Sensing of Cloud, Aerosol, and Water Vapor Properties from the Moderate Resolution Imaging Spectrometer (MODIS). *IEEE Transactions on Geoscience and Remote Sensing*, **30(1)**:2-27.
- Schläpfer D., 1998: *Differential Absorption Methodology for Imaging Spectroscopy of Atmospheric Water Vapor*. Remote Sensing Series, RSL, Zuerich, Vol. 32, pp. 131.